




Numerical solution for a fractional operator-based mathematical model of a brain tumour

Mallanagoud Mulimani¹ · S. Kumbinarasaiah¹ 

Received: 9 October 2023 / Accepted: 29 March 2024

© The Author(s), under exclusive licence to The Forum D'Analystes 2024

Abstract

Intricate mathematical models of malignant growths have been devised, particularly for solid tumours, whose growth is predominantly driven by cellular proliferation. The most severe type of brain cancer, gliomas, are distinguished by their extensive infiltration into nearby tissue. Glioma tumour growth is more aggressive than other types of cancer growth because of the diffusive behaviour of gliomas. The invasiveness of gliomas, however, necessitates a revision to incorporate cellular motility in addition to proliferative development. We examine some recent advances in the mathematical modelling of gliomas, and this study highlights how mathematical modelling can be used to create better glioblastoma multiforme (GBM) treatments. A simple two-dimensional mathematical model of glioma development and dissemination obtained from the fractional operator in terms of Caputo is the fractional Burgess equations (FBEs), which are expanded in this model. A newly introduced numerical algorithm based on an operational matrix extracted from the Taylor wavelets is described to find a solution for this model. This efficient numerical method transformed the given problem into a collection of algebraic equations. On solving these algebraic equations, we obtained the unknown coefficients. We found the solution to the given equation by substituting the unknown coefficients. Finally, three types of FBEs are used to simulate and test the suggested technique to verify its accuracy and superiority.

Keywords Fractional Burgess equations · Taylor wavelets · Collocation points · Operational matrix · Glioblastoma

Mathematics Subject Classification 26A33 · 35G25 · 49M15 · 65T60 · 65M70

Communicated by Muslim Malik.

✉ S. Kumbinarasaiah
kumbinarasaiah@gmail.com

¹ Department of Mathematics, Bangalore University, Bengaluru, India

1 Introduction

Due to the significance of its applications, fractional calculus is a trending research area. Fractional calculus has a long history that dates back more than 300 years. L'Hospital initially highlighted the issue of the fractional derivative of order $1/2$. Lagrange, Laplace, Euler, Bernoulli, and d'Alembert conducted the first studies of the partial differential equation (PDE) in the eighteenth century as an essential tool for understanding the physical properties of solids, fluids and, more widely, as the primary approach for analytical examination of real-world models in many fields. Fractional derivatives have recently received increased attention from scholars, particularly in light of their numerous uses in science, economics, engineering, and biology [1–3]. There has been a lot of interest in fractional calculus because it is employed in many disciplines, including control theory, biochemistry, electroanalytical chemistry, electrical circuits, thermodynamics, biophysics, blood flow phenomena, aerodynamics, and viscoelasticity [4–7]. There are many types of fractional operators available in the literature, such as Caputo [7], Grünwald–Laetnikov [7], Riemann–Liouville [7], Atangana–Baleanu [8], Caputo–Fabrizio [9]. Moreover, the theory of fractional differential equations and their applications has advanced significantly. On the other hand, fractional derivatives offer a crucial tool for defining inherited traits of various needs and therapies. Fractional differential equations have this essential benefit over traditional integer-order problems.

A robust analytical tool for examining biological issues, mathematical modelling enables the development and testing hypotheses that may improve comprehension of the biological process. A brain tumour is the growth of cells in the brain or close to it. Brain tumours can develop within or close to the brain tissue. Nerves, the pineal, the pituitary, and the membranes covering the brain's surface are nearby structures. A more invasive form of glioma in the brain is called glioblastoma, often known as GBM [10]. It is the most prevalent and dangerous brain tumour in people. Gliomas, which comprise around 50% of all primary brain tumours, are diffuse, highly invasive tumours of the brain [11]. From a medical standpoint, GBM is a rapidly growing tumour composed of poorly differentiated astrocytes that exhibit vascular proliferation, necrosis, pleomorphism, and high rates of mitosis. The prognosis for glioma patients is influenced by several factors, including their age, the grade and histologic type of the malignancy, and the extent of their neurological functioning [12]. However, the grade of malignancy contains at least two components—*invasiveness* and *net proliferation rate*—that can only be roughly defined histologically.

In contrast to solid tumours, which exhibit straightforward exponential or geometric growth that reflects the expansion of volume (equal to the total number of affected cells in the tumour), gliomas are made up of motile cells that can move and reproduce. The *invasiveness* makes it nearly impossible to quantify the growth rate as a standard volume-doubling time, even in the ideal scenario where at least two scans (CT, MRI) are analyzed at various periods without therapy intervening [13]. The line dividing the tumour from healthy tissue is unclear, and counting the number of cells in healthy tissue is impossible. New mathematical formulations are needed for

gliomas because it is practically impossible to measure the growth rate of gliomas or to determine the spatiotemporal infiltration of gliomas, which is essential to apply the results of more than two decades of surveys of mathematical formulations of other cancers. Although this glioma can develop at any age, it is more common in adults over the age of 45. They typically develop in the cerebral hemispheres but can also develop in the cerebellum. They can be viewed as having spherical geometry from a mathematical perspective, as shown in Fig. 1.

It is evident that gliomas are, in fact, physiologically malignant, given that even slowly developing gliomas are rarely curable by radical resection and that the average untreated survival duration for high-grade gliomas ranges from 6 months to 1 year [11]. They are not encapsulated in most cases, and even ependymomas that appear to be encapsulated cannot be treated with a simple resection [14]. These findings are consistent with the observation that individual glioma cells are incredibly mobile, capable of invading the majority of the rat neural axis in less than a week after implantation, and known to be viable even at great distances from the bulk lesion in people [15]. Gliomas can proliferate rapidly, with in vivo doubling times as low as one week [11].

Burgess and many others proposed a 3-dimensional mathematical model of a glioblastoma's unrestricted growth without medicinal treatments [16]. This model examines the dynamics of glioma proliferation-annihilation. However, it does not address the possibility that some tumour cell annihilation may manifest due to the administration of cancer-curing agents. This model contains data on the tumour's changing density at any spatiotemporal location. It is important to note that some two-dimensional mathematical models, such as those proposed in [17] and [18], before the fractional Burgess equation model. In the current work, we will develop a mathematical model that considers the impact of several cancericidal substances and, consequently, the potential to eradicate or significantly slow the growth of gliomas using the fractional operator. Numerous studies have examined the equation for tumour growth and characterized the original two-dimensional tumour model [10, 16–22]. The tumour growth is defined as

Fig. 1 Demonstration of a glioblastoma brain tumour in the parietal lobe



Glioblastoma Multiforme

Rate of change of tumour cell density = Growth of tumour cells
+ Diffusion of tumour cells,

and in mathematical terms,

$$\frac{\partial \Psi(r, \tau)}{\partial \tau} = g\Psi(r, \tau) + D\nabla^2\Psi(r, \tau).$$

These models take into account cell proliferation (g) and diffusion (D), the two key factors in the formation of an invading brain tumour, and integrate them into a reaction–diffusion equation [23]:

$$\frac{\partial \Psi(r, \tau)}{\partial \tau} = g\Psi(r, \tau) + D\frac{1}{r^2}\frac{\partial}{\partial r}\left(r^2\frac{\partial \Psi(r, \tau)}{\partial r}\right).$$

The tumour cells are thought to develop exponentially at a constant rate in these models. Owing to the significance of these models, it can occasionally be challenging to reach a solution. As a result, there is a lot of interest in developing methods for calculating approximations of solutions for these models.

When representing data or other functions, wavelets are mathematical functions that meet specific criteria. Since Joseph Fourier realized that sines and cosines could be superposed to describe other functions in the early 1800s, approximation utilizing the superposition of functions has been used. In the 1980s and 1990s, wavelets were created as an alternative to Fourier analysis of signals. Jean Morlet, Baroness Ingrid Daubechies, Alex Grossman, Palle Jorgensen, Yves Meyer, Ronald Coifman, Alfred Haar, and Stephane Mallat were a few key players in this invention. Yet, the scale at which we examine the data has a specific significance in wavelet analysis. Wavelet algorithms process different scales or resolutions of data. Wavelet transforms are extremely helpful for signal analysis, compression, and de-noising. Fourier analysis is impoverished at approximating sharp spikes when investigating its solutions; however, we can employ approximation functions that are tidily contained in finite domains appreciations to wavelet analysis. For estimating data with sharp discontinuities, wavelets work well. Compared to other methods, the wavelet approach gives better outcomes. Numerical methods based on wavelets are effective for solving PDEs. In the literature, some wavelet-based numerical techniques have been successfully solved, which are the Fibonacci wavelet method [24, 25], Legendre wavelet method [26], Chebyshev wavelet method [26], Bernoulli wavelet method [27–29], Haar wavelet technique [30], Euler wavelet collocation approach [31], Taylor wavelet method [32], Hermite wavelet collocation method [33], Laguerre wavelet collocation technique [33].

Taylor wavelets are compact, spatially oriented oscillatory functions that are the foundation for numerous significant spaces. Estimating the integrals using operational matrices can reduce the research problem to a set of algebraic equations utilizing the wavelet basis. The Taylor wavelet collocation method (TWCM) demonstrates many beneficial traits: compared to Chebyshev, Fibonacci, Legendre, Laguerre, and Bernoulli wavelets, these techniques have high accuracy, the potential to be implemented quickly and are more straightforward and less expensive to

compute. In our review of the literature, we found the following excellent papers regarding the Taylor wavelet approach: fractional delay differential equations [34], systems of nonlinear fractional differential equations [35], fractional integrodifferential equations [36], generalized Burgers-Huxley equation [37], Bratu-type equations [38], Lane-Emden equations [39], and time-fractional telegraph equations [40]. In this study, we have generated an operational matrix of integration using Taylor wavelets and developed a novel approach called TWCM. Some of them are solved fractional order brain tumour models using a few methods in the literature, including the generalized Lagurre wavelet-based method [41], orthonormal Bernoulli polynomials-based method [42], finite difference method [43], predictor–corrector method [44], and shifted fractional-order Legendre–Gauss–Radau collocation method [45]. As of our literature survey, no one considered the brain tumour model called FBE by Taylor wavelets. This compels us to study this model by TWCM. Many semi-analytical methods depend on controlling parameters, but the proposed approach is free from that.

The paper is organized as described in the paragraph that follows. The fractional derivative, Taylor wavelets, function approximation, and their operational integration matrix are covered in Sect. 2. The mathematical model of gliomas is explained in Sect. 3. Some theorems on convergence analysis are illustrated in Sect. 4. The proposed technique TWCM is formulated in Sect. 5. Implementation of test problems is available in Sect. 6. The conclusion is enclosed with concluding remarks in Sect. 7.

2 Preliminaries

2.1 Caputo fractional derivative

The Caputo fractional order derivative of $f(t) \in C_\mu$ is defined by [46],

$$\frac{\partial^\alpha f(t)}{\partial t^\alpha} = \frac{1}{\Gamma(m - \alpha)} \int_0^t (t - x)^{m-\alpha-1} \frac{\partial^m f(x)}{\partial x^m} dx,$$

for $m - 1 < \alpha \leq m$, where $m = [\alpha]$ be a positive integer, $t > 0, f(t) \in C_\mu^m, \mu \geq -1$.

2.2 Wavelets and Taylor wavelets

The family of functions known as wavelets are descended from a single function called the mother wavelet through dilatation and translation. When the translation parameter q and the dilation parameter p are continuously variable, we have the family of continuous wavelets shown in [24].

$$\omega_{p,q}(t) = |p|^{-\frac{1}{2}} \omega\left(\frac{t - q}{p}\right), \quad p, q \in \mathbb{R}, p \neq 0.$$

It introduces the discrete wavelet family as if $p = p_0^{-k}, q = nq_0 p_0^{-k}, p_0 > 1, q_0 > 1$, and k and n are positive integers.

$$\omega_{k,n}(t) = |p_0^{-k}|^{\frac{1}{2}} \omega\left(\frac{t - nq_0 p_0^{-k}}{p_0^{-k}}\right) = |p_0|^{\frac{k}{2}} \omega(p_0^k t - nq_0),$$

where $\omega_{k,n}(t)$ is a wavelet basis for $L^2(\mathbb{R})$.

Taylor wavelets $\omega_{n,m}(t) = \omega(k, n, m, t)$ involve four arguments; $n = 1, 2, \dots, 2^{k-1}$, m is the degree of Taylor polynomials, t is the normalized time, and k is any positive integer. On the interval $[0, 1)$, Taylor wavelets are defined as [34–36],

$$\omega_{n,m}(t) = \begin{cases} 2^{\frac{k-1}{2}} \tilde{T}_m(2^{k-1}t - n + 1), & \frac{n-1}{2^{k-1}} \leq t < \frac{n}{2^{k-1}}, \\ 0, & \text{Otherwise,} \end{cases}$$

with

$$\tilde{T}_m(t) = \sqrt{2m+1} T_m(t),$$

where $n = 1, 2, \dots, 2^{k-1}$ and $m = 0, 1, 2, \dots, M-1$. The coefficient $\sqrt{2m+1}$ is for normality, the dilation parameter is $p = 2^{-(k-1)}$ and the translation parameter $q = \hat{n}2^{-(k-1)}$. $T_m(t)$ is the Taylor polynomial of degree m and it can be expressed as $T_m(t) = t^m$. $\tilde{T}_m(t)$ is the normal Taylor polynomial of degree m .

2.3 Function approximation

The Taylor wavelets can be used to expand a function $f(t) \in L^2[0, 1]$ as follows:

$$f(t) = \sum_{n=1}^{\infty} \sum_{m=0}^{\infty} c_{n,m} \omega_{n,m}(t).$$

The above infinite series can be truncated to finite series for $f(t)$ as

$$f(t) = \sum_{n=1}^{2^{k-1}} \sum_{m=0}^{M-1} c_{n,m} \omega_{n,m}(t) = A^T \omega(t),$$

where T denotes the transposition and A , $\omega(t)$ are $2^{k-1}M \times 1$ matrices given by

$$A^T = [c_{1,0}, \dots, c_{1,M-1}, c_{2,0}, \dots, c_{2,M-1}, \dots, c_{2^{k-1},0}, \dots, c_{2^{k-1},M-1}],$$

$$\omega(t) = [\omega_{1,0}(t), \dots, \omega_{1,M-1}(t), \omega_{2,0}(t), \dots, \omega_{2,M-1}(t), \dots, \omega_{2^{k-1},0}(t), \dots, \omega_{2^{k-1},M-1}(t)]^T.$$

Let $\{\omega_{n,m}\}$ be the Taylor wavelet sequence, $n = 1, 2, \dots$, and $m = 0, 1, \dots$. The components of the sequence $\{\omega_{n,m}\}$ span a Taylor wavelet space for every fixed n . $L(\{\omega_{n,m}\}) = L^2[0, 1]$ is Banach space.

2.4 Operational matrix of integration

We have simplified a few Taylor wavelet basis here at $k = 1$:

$$\begin{aligned} \omega_{1,0}(t) &= 1, \\ \omega_{1,1}(t) &= \sqrt{3}t, \\ \omega_{1,2}(t) &= \sqrt{5}t^2, \\ \omega_{1,3}(t) &= \sqrt{7}t^3, \\ \omega_{1,4}(t) &= 3t^4, \\ \omega_{1,5}(t) &= \sqrt{11}t^5, \\ \omega_{1,6}(t) &= \sqrt{13}t^6, \\ \omega_{1,7}(t) &= \sqrt{15}t^7, \\ \omega_{1,8}(t) &= \sqrt{17}t^8, \\ \omega_{1,9}(t) &= \sqrt{19}t^9, \\ \omega_{1,10}(t) &= \sqrt{21}t^{10}, \\ \omega_{1,11}(t) &= \sqrt{23}t^{11}, \end{aligned}$$

and,

$$\omega_{10}(t) = [\omega_{1,0}(t), \omega_{1,1}(t), \omega_{1,2}(t), \omega_{1,3}(t), \omega_{1,4}(t), \omega_{1,5}(t), \omega_{1,6}(t), \omega_{1,7}(t), \omega_{1,8}(t), \omega_{1,9}(t)]^T.$$

By integrating the basis mentioned above with respective t from 0 and t and then expressing integrated wavelet basis as a linear combination is given by;

$$\begin{aligned} \int_0^t \omega_{1,0}(t)dt &= \left[0 \quad \frac{1}{\sqrt{3}} \quad 0 \quad 0 \quad 0 \quad 0 \quad 0 \quad 0 \quad 0 \quad 0 \right] \omega_{10}(t), \\ \int_0^t \omega_{1,1}(t)dt &= \left[0 \quad 0 \quad \frac{\sqrt{3}}{2\sqrt{5}} \quad 0 \quad 0 \quad 0 \quad 0 \quad 0 \quad 0 \quad 0 \right] \omega_{10}(t), \end{aligned}$$

$$\int_0^t \omega_{1,2}(t) dt = \begin{bmatrix} 0 & 0 & 0 & \frac{\sqrt{5}}{3\sqrt{7}} & 0 & 0 & 0 & 0 & 0 & 0 \end{bmatrix} \omega_{10}(t),$$

$$\int_0^t \omega_{1,3}(t) dt = \begin{bmatrix} 0 & 0 & 0 & 0 & \frac{\sqrt{7}}{12} & 0 & 0 & 0 & 0 & 0 \end{bmatrix} \omega_{10}(t),$$

$$\int_0^t \omega_{1,4}(t) dt = \begin{bmatrix} 0 & 0 & 0 & 0 & 0 & \frac{3}{5\sqrt{11}} & 0 & 0 & 0 & 0 \end{bmatrix} \omega_{10}(t),$$

$$\int_0^t \omega_{1,5}(t) dt = \begin{bmatrix} 0 & 0 & 0 & 0 & 0 & 0 & \frac{\sqrt{11}}{6\sqrt{13}} & 0 & 0 & 0 \end{bmatrix} \omega_{10}(t),$$

$$\int_0^t \omega_{1,6}(t) dt = \begin{bmatrix} 0 & 0 & 0 & 0 & 0 & 0 & 0 & \frac{\sqrt{13}}{7\sqrt{15}} & 0 & 0 \end{bmatrix} \omega_{10}(t),$$

$$\int_0^t \omega_{1,7}(t) dt = \begin{bmatrix} 0 & 0 & 0 & 0 & 0 & 0 & 0 & 0 & \frac{\sqrt{15}}{8\sqrt{17}} & 0 \end{bmatrix} \omega_{10}(t),$$

$$\int_0^t \omega_{1,8}(t) dt = \begin{bmatrix} 0 & 0 & 0 & 0 & 0 & 0 & 0 & 0 & 0 & \frac{\sqrt{17}}{9\sqrt{19}} \end{bmatrix} \omega_{10}(t),$$

$$\int_0^t \omega_{1,9}(t) dt = [0 \ 0 \ 0 \ 0 \ 0 \ 0 \ 0 \ 0 \ 0 \ 0] \omega_{10}(t) + \frac{\sqrt{19}}{10\sqrt{21}} \omega_{1,10}(t).$$

Hence,

$$\int_0^t \omega(t) dt = H_{10 \times 10} \omega_{10}(t) + \overline{\omega_{10}(t)},$$

where,

$$H_{10 \times 10} = \begin{bmatrix} 0 & \frac{1}{\sqrt{3}} & 0 & 0 & 0 & 0 & 0 & 0 & 0 & 0 \\ 0 & 0 & \frac{\sqrt{3}}{2\sqrt{5}} & 0 & 0 & 0 & 0 & 0 & 0 & 0 \\ 0 & 0 & 0 & \frac{\sqrt{5}}{3\sqrt{7}} & 0 & 0 & 0 & 0 & 0 & 0 \\ 0 & 0 & 0 & 0 & \frac{\sqrt{7}}{12} & 0 & 0 & 0 & 0 & 0 \\ 0 & 0 & 0 & 0 & 0 & \frac{3}{5\sqrt{11}} & 0 & 0 & 0 & 0 \\ 0 & 0 & 0 & 0 & 0 & 0 & \frac{\sqrt{11}}{6\sqrt{13}} & 0 & 0 & 0 \\ 0 & 0 & 0 & 0 & 0 & 0 & 0 & \frac{\sqrt{13}}{7\sqrt{15}} & 0 & 0 \\ 0 & 0 & 0 & 0 & 0 & 0 & 0 & 0 & \frac{\sqrt{15}}{8\sqrt{17}} & 0 \\ 0 & 0 & 0 & 0 & 0 & 0 & 0 & 0 & 0 & \frac{\sqrt{17}}{9\sqrt{19}} \\ 0 & 0 & 0 & 0 & 0 & 0 & 0 & 0 & 0 & 0 \end{bmatrix}$$

$$\text{and } \overline{\omega}_{10}(t) = \begin{bmatrix} 0 \\ 0 \\ 0 \\ 0 \\ 0 \\ 0 \\ 0 \\ 0 \\ 0 \\ 0 \\ \frac{\sqrt{19}}{10\sqrt{21}} \omega_{1,10}(t) \end{bmatrix}.$$

The generalized first integration of n -wavelet basis is denoted as:

$$\int_0^t \omega(t) dt = H_{n \times n} \omega(t) + \overline{\omega}(t),$$

where,

$$H_{n \times n} = \begin{bmatrix} 0 & \frac{1}{\sqrt{3}} & 0 & 0 & 0 & \dots & 0 & 0 \\ 0 & 0 & \frac{\sqrt{3}}{2\sqrt{5}} & 0 & 0 & \dots & 0 & 0 \\ 0 & 0 & 0 & \frac{\sqrt{5}}{3\sqrt{7}} & 0 & \dots & 0 & 0 \\ 0 & 0 & 0 & 0 & \frac{\sqrt{7}}{12} & \dots & 0 & 0 \\ \vdots & \vdots & \vdots & \vdots & \ddots & \ddots & 0 & 0 \\ 0 & 0 & 0 & 0 & 0 & 0 & \frac{\sqrt{2(n-2)+1}}{(n-1)\sqrt{2(n-2)+3}} & 0 \\ 0 & 0 & 0 & 0 & 0 & \dots & 0 & \frac{\sqrt{2(n-1)+1}}{n\sqrt{2(n-1)+3}} \\ 0 & 0 & 0 & 0 & 0 & \dots & 0 & 0 \end{bmatrix}$$

and $\overline{\omega_n(t)} = \begin{bmatrix} 0 \\ 0 \\ 0 \\ 0 \\ 0 \\ 0 \\ \vdots \\ \frac{\sqrt{2n-1}}{n\sqrt{2n+1}} \omega_{1,n}(t) \end{bmatrix}$.

Integrate the above basis once again. Then we have,

$$\int_0^t \int_0^t \omega_{1,0}(t) dt dt = \begin{bmatrix} 0 & 0 & \frac{1}{2\sqrt{5}} & 0 & 0 & 0 & 0 & 0 & 0 & 0 \end{bmatrix} \omega_{10}(t),$$

$$\int_0^t \int_0^t \omega_{1,1}(t) dt dt = \begin{bmatrix} 0 & 0 & 0 & \frac{1}{2\sqrt{21}} & 0 & 0 & 0 & 0 & 0 & 0 \end{bmatrix} \omega_{10}(t),$$

$$\int_0^t \int_0^t \omega_{1,2}(t) dt dt = \begin{bmatrix} 0 & 0 & 0 & 0 & \frac{\sqrt{5}}{36} & 0 & 0 & 0 & 0 & 0 \end{bmatrix} \omega_{10}(t),$$

$$\int_0^t \int_0^t \omega_{1,3}(t) dt dt = \begin{bmatrix} 0 & 0 & 0 & 0 & 0 & \frac{\sqrt{7}}{20\sqrt{11}} & 0 & 0 & 0 & 0 \end{bmatrix} \omega_{10}(t),$$

$$\int_0^t \int_0^t \omega_{1,4}(t) dt dt = \begin{bmatrix} 0 & 0 & 0 & 0 & 0 & 0 & \frac{1}{10\sqrt{13}} & 0 & 0 & 0 \end{bmatrix} \omega_{10}(t),$$

$$\int_0^t \int_0^t \omega_{1,5}(t) dt dt = \left[0 \ 0 \ 0 \ 0 \ 0 \ 0 \ 0 \ 0 \ \frac{\sqrt{11}}{42\sqrt{15}} \ 0 \ 0 \right] \omega_{10}(t),$$

$$\int_0^t \int_0^t \omega_{1,6}(t) dt dt = \left[0 \ 0 \ 0 \ 0 \ 0 \ 0 \ 0 \ 0 \ 0 \ \frac{\sqrt{13}}{56\sqrt{17}} \ 0 \right] \omega_{10}(t),$$

$$\int_0^t \int_0^t \omega_{1,7}(t) dt dt = \left[0 \ 0 \ 0 \ 0 \ 0 \ 0 \ 0 \ 0 \ 0 \ 0 \ \frac{\sqrt{5}}{24\sqrt{57}} \right] \omega_{10}(t),$$

$$\int_0^t \int_0^t \omega_{1,8}(t) dt dt = [0 \ 0 \ 0 \ 0 \ 0 \ 0 \ 0 \ 0 \ 0 \ 0 \ 0] \omega_{10}(t) + \frac{\sqrt{17}}{90\sqrt{21}} \omega_{1,10}(t),$$

$$\int_0^t \int_0^t \omega_{1,9}(t) dt dt = [0 \ 0 \ 0 \ 0 \ 0 \ 0 \ 0 \ 0 \ 0 \ 0 \ 0] \omega_{10}(t) + \frac{\sqrt{19}}{110\sqrt{23}} \omega_{1,11}(t).$$

Hence,

$$\int_0^t \int_0^t \omega(t) dt dt = H'_{10 \times 10} \omega_{10}(t) + \overline{\omega_{10}(t)},$$

where

$$H'_{10 \times 10} = \begin{bmatrix} 0 & 0 & \frac{1}{2\sqrt{5}} & 0 & 0 & 0 & 0 & 0 & 0 & 0 & 0 \\ 0 & 0 & 0 & \frac{1}{2\sqrt{21}} & 0 & 0 & 0 & 0 & 0 & 0 & 0 \\ 0 & 0 & 0 & 0 & \frac{\sqrt{5}}{36} & 0 & 0 & 0 & 0 & 0 & 0 \\ 0 & 0 & 0 & 0 & 0 & \frac{\sqrt{7}}{20\sqrt{11}} & 0 & 0 & 0 & 0 & 0 \\ 0 & 0 & 0 & 0 & 0 & 0 & \frac{1}{10\sqrt{13}} & 0 & 0 & 0 & 0 \\ 0 & 0 & 0 & 0 & 0 & 0 & 0 & \frac{\sqrt{11}}{42\sqrt{15}} & 0 & 0 & 0 \\ 0 & 0 & 0 & 0 & 0 & 0 & 0 & 0 & \frac{\sqrt{13}}{56\sqrt{17}} & 0 & 0 \\ 0 & 0 & 0 & 0 & 0 & 0 & 0 & 0 & 0 & \frac{\sqrt{5}}{24\sqrt{57}} & 0 \\ 0 & 0 & 0 & 0 & 0 & 0 & 0 & 0 & 0 & 0 & 0 \\ 0 & 0 & 0 & 0 & 0 & 0 & 0 & 0 & 0 & 0 & 0 \end{bmatrix}$$

$$\text{and } \overline{\omega_{10}(t)}' = \begin{bmatrix} 0 \\ 0 \\ 0 \\ 0 \\ 0 \\ 0 \\ 0 \\ 0 \\ \frac{\sqrt{17}}{90\sqrt{21}}\omega_{1,10}(t) \\ \frac{\sqrt{19}}{110\sqrt{23}}\omega_{1,11}(t) \end{bmatrix}.$$

In this way, we can generate the matrices for our convenience.

3 The mathematical model of gliomas

Based on the examination of serial CT scans taken in the final year of a patient with recurrent anaplastic astrocytoma, many researchers [10, 16–22] created a mathematical model of glioma growth and diffusion. The model explained the gradual development of the glioma cell population exclusively by diffusion and proliferation, which can be read in words.

Rate of change of tumour cell density = Growth of tumour cells
+ Diffusion of tumour cells,

and in mathematical terms,

$$\frac{\partial \Psi(r, \tau)}{\partial \tau} = g\Psi(r, \tau) + D\nabla^2\Psi(r, \tau) = g\Psi(r, \tau) + D\frac{1}{r^2}\frac{\partial}{\partial r}\left(r^2\frac{\partial \Psi(r, \tau)}{\partial r}\right), \quad (3.1)$$

where $\partial_\tau \Psi(r, \tau) = \frac{\partial \Psi(r, \tau)}{\partial \tau}$. $\Psi(r, \tau)$ is the cell density at radius r , and time τ . g , stands for the net rate of cell growth and is described as a decimal fraction of each day. ∇^2 is the Laplacian operator. The diffusion coefficient, D , is measured in cm^2 per day. The researchers [21, 22, 41] modified the model above to include a killing term in Eq. (3.1).

Rate of change of tumour cell density = Growth of tumour cells
+ Diffusion of tumour cells
– Killing rate of tumour cells.

This can be written in mathematical form

$$\frac{\partial \Psi(r, \tau)}{\partial \tau} = g\Psi(r, \tau) + D\frac{1}{r^2}\frac{\partial}{\partial r}\left(r^2\frac{\partial \Psi(r, \tau)}{\partial r}\right) - k_\tau\Psi(r, \tau), \quad (3.2)$$

k_τ is the killing rate of tumour cells. The Eq. (3.2) can be written in the form as

$$\frac{\partial \Psi(r, \tau)}{\partial \tau} = \Psi(r, \tau)(g - k_\tau) + D \left(\frac{\partial^2 \Psi(r, \tau)}{\partial r^2} + \frac{2}{r} \frac{\partial \Psi(r, \tau)}{\partial r} \right). \tag{3.3}$$

Assume that $t = 2D\tau$, and differentiate then

$$\begin{aligned} \partial t &= 2D\partial \tau, \\ \frac{\partial \tau}{\partial t} &= \frac{1}{2D}. \end{aligned} \tag{3.4}$$

Assume that $\Phi(r, t) = r\Psi(r, \tau)$ and differentiate concerning with t and r , then

$$\frac{\partial \Phi(r, t)}{\partial t} = r \frac{\partial \Psi(r, \tau)}{\partial t} = r \frac{\partial \Psi(r, \tau)}{\partial \tau} \frac{\partial \tau}{\partial t} = \frac{r}{2D} \frac{\partial \Psi(r, \tau)}{\partial \tau}, \tag{3.5}$$

and

$$\frac{\partial \Phi(r, t)}{\partial r} = r \frac{\partial \Psi(r, \tau)}{\partial r} + \Psi(r, \tau). \tag{3.6}$$

Again, differentiate Eq. (3.5), and we get

$$\frac{\partial^2 \Phi(r, t)}{\partial r^2} = r \frac{\partial^2 \Psi(r, \tau)}{\partial r^2} + 2 \frac{\partial \Psi(r, \tau)}{\partial r}. \tag{3.7}$$

Equations (3.5), (3.6), and (3.7) can be written as

$$\frac{\partial \Psi(r, \tau)}{\partial \tau} = \frac{2D}{r} \frac{\partial \Phi(r, t)}{\partial t}, \tag{3.8}$$

$$\frac{\partial \Psi(r, \tau)}{\partial r} = \frac{1}{r} \left(\frac{\partial \Phi(r, t)}{\partial r} - \Psi(r, \tau) \right), \tag{3.9}$$

$$\frac{\partial^2 \Psi(r, \tau)}{\partial r^2} = \frac{1}{r} \left(\frac{\partial^2 \Phi(r, t)}{\partial r^2} - 2 \frac{\partial \Psi(r, \tau)}{\partial r} \right). \tag{3.10}$$

By substituting the Eqs. (3.8), (3.9), and (3.10) in (3.3), then

$$\frac{\partial \Phi(r, t)}{\partial t} = \frac{g - k_\tau}{2D} \Phi(r, t) + \frac{1}{2} \frac{\partial^2 \Phi(r, t)}{\partial r^2}. \tag{3.11}$$

If $\Theta(r, t) = \frac{g - k_\tau}{2D} \Phi(r, t)$ and $\Phi(r, t_0)$ is the initial growth profile, then

$$\frac{\partial \Phi(r, t)}{\partial t} = \Theta(r, t) + \frac{1}{2} \frac{\partial^2 \Phi(r, t)}{\partial r^2},$$

$$\Phi(r, t_0) = \zeta(r).$$

You can write the fractional Burgess equation as

$$\frac{\partial^\alpha \Phi(r, t)}{\partial t^\alpha} = \Theta(r, t) + \frac{1}{2} \frac{\partial^2 \Phi(r, t)}{\partial r^2}, \quad (3.12)$$

with initial condition

$$\Phi(r, t_0) = \zeta(r).$$

The Caputo derivative operator of order $0 < \alpha \leq 1$ is represented by the symbol α .

4 Some theorems on the convergence analysis

Theorem 1 Let $\Phi(r, t)$ in $L^2(\mathbb{R} \times \mathbb{R})$ be a continuous bounded function defined on $[0, 1] \times [0, 1]$, then Taylor wavelet expansion of $\Phi(r, t)$ is uniformly converges to it.

Proof Let $\Phi(r, t)$ in $L^2(\mathbb{R} \times \mathbb{R})$ be a continuous function defined on $[0, 1] \times [0, 1]$ and bounded by a real number μ . The approximation of $\Phi(r, t)$ is;

$$\Phi(r, t) = \sum_{n=1}^{\infty} \sum_{m=0}^{\infty} a_{n,m} \omega_{n,m}(r) \omega_{n,m}(t),$$

where, $a_{n,m} = \langle \Phi(r, t), \omega_{n,m}(r) \omega_{n,m}(t) \rangle$, and $\langle \cdot, \cdot \rangle$ represents inner product. Since $\omega_{i,j}(r) \omega_{i,j}(t)$ are orthogonal functions on $[0, 1]$. Then,

$$a_{n,m} = \int_0^1 \int_0^1 \Phi(r, t) \omega_{n,m}(r) \omega_{n,m}(t) dr dt,$$

$$a_{n,m} = \int_0^1 \int_I \Phi(r, t) 2^{\frac{k-1}{2}} \sqrt{2m+1} T_m(2^{k-1}r - n + 1) \omega_{n,m}(t) dr dt,$$

where $I = \left[\frac{n-1}{2^{k-1}}, \frac{n}{2^{k-1}} \right]$. Put $2^{k-1}r - n + 1 = x$ then,

$$a_{n,m} = 2^{\frac{k-1}{2}} \sqrt{2m+1} \int_0^1 \int_0^1 \Phi\left(\frac{x-1+n}{2^{k-1}}, t\right) T_m(x) \frac{dx}{2^{k-1}} \omega_{n,m}(t) dt,$$

$$a_{n,m} = 2^{-\left(\frac{k-1}{2}\right)} \sqrt{2m+1} \int_0^1 \left[\int_0^1 \Phi\left(\frac{x-1+n}{2^{k-1}}, t\right) T_m(x) dx \right] \omega_{n,m}(t) dt.$$

By generalized mean value theorem for integrals,

$$a_{n,m} = 2^{-\left(\frac{k-1}{2}\right)} \sqrt{2m+1} \int_0^1 \Phi\left(\frac{\xi-1+n}{2^{k-1}}, t\right) \omega_{n,m}(t) dt \left[\int_0^1 T_m(x) dx \right],$$

where $\xi \in (0, 1)$ and choose $\int_0^1 T_m(x) dx = A$,

$$a_{n,m} = A 2^{-\left(\frac{k-1}{2}\right)} \sqrt{2m+1} \int_{\frac{n-1}{2^{k-1}}}^{\frac{n}{2^{k-1}}} \Phi\left(\frac{\xi-1+n}{2^{k-1}}, t\right) 2^{\frac{k-1}{2}} \sqrt{2m+1} T_m(2^{k-1}t - n + 1) dt,$$

$$a_{n,m} = A(2m+1) \int_{\frac{n-1}{2^{k-1}}}^{\frac{n}{2^{k-1}}} \Phi\left(\frac{\xi-1+n}{2^{k-1}}, t\right) T_m(2^{k-1}t - n + 1) dt.$$

Put $2^{k-1}t - n + 1 = x$ then,

$$a_{n,m} = A(2m+1) \int_0^1 \Phi\left(\frac{\xi-1+n}{2^{k-1}}, \frac{x-1+n}{2^{k-1}}\right) T_m(x) \frac{dx}{2^{k-1}},$$

$$a_{n,m} = A(2m+1) 2^{-k+1} \int_0^1 \Phi\left(\frac{\xi-1+n}{2^{k-1}}, \frac{x-1+n}{2^{k-1}}\right) T_m(x) dx.$$

By generalized mean value theorem for integrals,

$$a_{n,m} = A 2^{-k+1} \Phi\left(\frac{\xi-1+n}{2^{k-1}}, \frac{\xi_1-1+n}{2^{k-1}}\right) \int_0^1 P_m(x) dx,$$

where, $\xi_1 \in (0, 1)$ and $\int_0^1 P_m(x) dx = B$ then

$$a_{n,m} = AB(2m+1) 2^{-k+1} \Phi\left(\frac{\xi-1+n}{2^{k-1}}, \frac{\xi_1-1+n}{2^{k-1}}\right), \forall \xi, \xi_1 \in (0, 1).$$

Therefore,

$$|a_{n,m}| = |AB(2m+1) 2^{-k+1}| \left| \Phi\left(\frac{\xi-1+n}{2^{k-1}}, \frac{\xi_1-1+n}{2^{k-1}}\right) \right|.$$

Since Φ is bounded by μ ,

$$|a_{n,m}| \leq |A||B||2m + 1||2^{-k+1}|\mu.$$

Therefore $\sum_{n=1}^{\infty} \sum_{m=0}^{\infty} a_{n,m}$ is absolutely convergent. Hence, the Taylor wavelet expansion of $\Phi(r, t)$ converges uniformly.

Theorem 2 [24] *Let the Taylor wavelet sequence $\{\omega_{n,m}^k(t)\}_{k=1}^{\infty}$ which are continuous functions defined in $L^2(\mathbb{R})$ in t on $[a, b]$ converges to the function $\omega(t)$ in $L^2(\mathbb{R})$ uniformly in t on $[a, b]$. Then $\omega(t)$ is continuous in $L^2(\mathbb{R})$ in t on $[a, b]$.*

Theorem 3 [24] *Let the Taylor wavelet sequence $\{\omega_{n,m}^k(t)\}_{k=1}^{\infty}$ converges itself in $L_2(\mathbb{R})$ uniformly in t on $[a, b]$. Then, there is a function $\omega(t)$ is continuous in $L_2(\mathbb{R})$ in t on $[a, b]$ and $\lim_{k \rightarrow \infty} \omega_{n,m}^k(r, t) = \omega(t) \forall t \in [a, b]$.*

Theorem 4 [25] *Let $\{r_i = t_i/i = 1, 2, \dots, 2^{k-1}M^2\}$ be any set of $\frac{2i-1}{2^k M^2}$ distinct points in $[a, b]$ and $\Phi(r, t) \in c[a, b]$, where $c[a, b]$ is a set of all continuous functions defined in $[a, b]$. $\Phi(r, t)$ be the solution of the given partial differential equation; then there is exactly one linear combination $\varphi(r, t)$ of polynomial-based wavelet functions that satisfy the.*

$$\Phi(r_i, t_i) = \varphi(r_i, t_i) \forall i = 1, 2, \dots, 2^{k-1}M^2.$$

5 Solution of a model

The primary goal of this part is to introduce a novel method based on Taylor wavelets for solving the Burgess equation. Consider the fractional linear/nonlinear PDE of the following type:

$$\frac{\partial^\alpha \Phi(r, t)}{\partial t^\alpha} = \Theta(r, t) + \frac{1}{2} \frac{\partial^2 \Phi(r, t)}{\partial r^2}, \tag{5.1}$$

where r, t are the independent variables, and Φ is a dependent variable with the given physical conditions.

$$\Phi(r, 0) = G_1(r), \Phi(0, t) = G_2(t), \Phi(c, t) = G_3(t), \tag{5.2}$$

where c be any constant, $G_1(r), G_2(t)$, and $G_3(t)$ are the real-valued and continuous functions. Let's assume,

$$\frac{\partial^3 \Phi(r, t)}{\partial r^2 \partial t} \approx \omega^T(r) Q \omega(t), \tag{5.3}$$

where, $\omega^T(r) = [\omega_{1,0}(r), \dots, \omega_{1,M-1}(r), \dots, \omega_{2^{k-1},0}(r), \dots, \omega_{2^{k-1},M-1}(r)]$,
 $Q = [b_{i,j}]$ be $2^{k-1}M \times 2^{k-1}M$ unknown matrix such that $i, j = 1, \dots, 2^{k-1}M$, and

$$\omega(t) = \left[\omega_{1,0}(t), \dots, \omega_{1,M-1}(t), \dots, \omega_{2^{k-1},0}(t), \dots, \omega_{2^{k-1},M-1}(t) \right]^T.$$

By integrating Eq. (5.3) concerning t from limit 0 to t .

$$\frac{\partial^2 \Phi(r, t)}{\partial r^2} = \frac{\partial^2 \Phi(r, 0)}{\partial r^2} + \omega^T(r) Q [H\omega(t) + \overline{\omega(t)}]. \tag{5.4}$$

Now integrate Eq. (5.4) twice concerning to r from 0 to r .

$$\frac{\partial \Phi(r, t)}{\partial r} = \frac{\partial \Phi(0, t)}{\partial r} + \frac{\partial \Phi(r, 0)}{\partial r} - \frac{\partial \Phi(0, 0)}{\partial r} + [H\omega(r) + \overline{\omega(r)}]^T Q [H\omega(t) + \overline{\omega(t)}], \tag{5.5}$$

$$\begin{aligned} \Phi(r, t) = & \Phi(0, t) + \Phi(r, 0) - \Phi(0, 0) + r \left[\frac{\partial \Phi(0, t)}{\partial r} - \frac{\partial \Phi(0, 0)}{\partial r} \right] \\ & + [H'\omega(r) + \overline{\omega(r)}]^T Q [H\omega(t) + \overline{\omega(t)}]. \end{aligned} \tag{5.6}$$

Put $r = c$ in Eq. (5.6) along with the given physical conditions in Eq. (5.2). We attain,

$$\begin{aligned} G_3(t) = & G_2(t) + G_1(c) - G_1(0) + c \left[\frac{\partial \Phi(0, t)}{\partial r} - \frac{\partial \Phi(0, 0)}{\partial r} \right] \\ & + \lim_{r \rightarrow c} [H'\omega(r) + \overline{\omega(r)}]^T Q [H\omega(t) + \overline{\omega(t)}], \end{aligned}$$

$$\begin{aligned} & \left[\frac{\partial \Phi(0, t)}{\partial r} - \frac{\partial \Phi(0, 0)}{\partial r} \right] \\ = & \frac{1}{c} \left[G_3(t) - G_2(t) - G_1(c) + G_1(0) - \lim_{r \rightarrow c} [H'\omega(r) + \overline{\omega(r)}]^T Q [H\omega(t) + \overline{\omega(t)}] \right]. \end{aligned} \tag{5.7}$$

Substitute Eq. (5.7) in Eqs. (5.5) and (5.6)

$$\begin{aligned} \frac{\partial \Phi(r, t)}{\partial r} = & \frac{\partial G_1(r)}{\partial r} \\ & + \frac{1}{c} \left[G_3(t) - G_2(t) - G_1(c) + G_1(0) - \lim_{r \rightarrow c} [H'\omega(r) + \overline{\omega(r)}]^T Q [H\omega(t) + \overline{\omega(t)}] \right] \\ & + [H\omega(r) + \overline{\omega(r)}]^T Q [H\omega(t) + \overline{\omega(t)}], \end{aligned} \tag{5.8}$$

$$\begin{aligned} \Phi(r, t) = & G_2(t) + G_1(r) - G_1(0) + [H'\omega(r) + \overline{\omega(r)}]^T Q [H\omega(t) + \overline{\omega(t)}] \\ & + \frac{r}{c} \left[G_3(t) - G_2(t) - G_1(c) + G_1(0) - \lim_{r \rightarrow c} [H'\omega(r) + \overline{\omega(r)}]^T Q [H\omega(t) + \overline{\omega(t)}] \right]. \end{aligned} \tag{5.9}$$

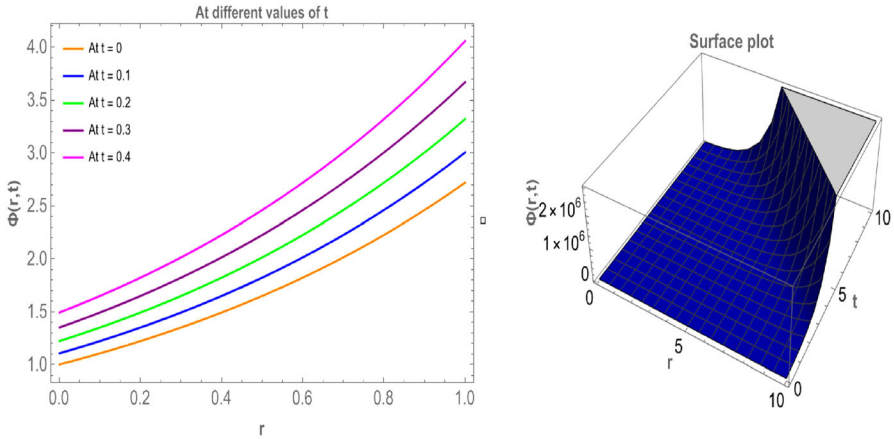


Fig. 2 The development of tumour cells in exponential form, for example, 1

Case I: If $\alpha = 1$ in Eq. (5.1), then differentiate Eq. (5.9) with concerning t . We obtain,

$$\begin{aligned} \frac{\partial \Phi(r, t)}{\partial t} &= \frac{d}{dt} G_2(t) + \frac{d}{dt} \left[\left[H' \omega(r) + \overline{\omega(r)} \right]^T Q \left[H \omega(t) + \overline{\omega(t)} \right] \right] \\ &+ \frac{r}{c} \frac{d}{dt} \left[G_3(t) - G_2(t) - G_1(c) + G_1(0) - \lim_{r \rightarrow c} \left[H' \omega(r) + \overline{\omega(r)} \right]^T Q \left[H \omega(t) + \overline{\omega(t)} \right] \right]. \end{aligned} \tag{5.10}$$

Now fit the $\Phi, \Phi_t, \Phi_r,$ and Φ_{rr} into Eq. (5.1), and discretise with their respective collocation points in Eq. (5.11).

Table 1 Projected method solution for the different α values at $r = 1$, for example, 1

t	TWCM				
	$\alpha = 0.6$	$\alpha = 0.7$	$\alpha = 0.8$	$\alpha = 0.9$	$\alpha = 1$
0.1	2.85512798	2.91016960	2.94982230	2.98012183	3.00416602
0.2	3.12723524	3.19387211	3.24426445	3.28521433	3.32011692
0.3	3.53776574	3.57255152	3.60477042	3.63672148	3.66929666
0.4	4.09021420	4.04970251	4.03483491	4.03813797	4.05519996
0.5	4.78844287	4.62918735	4.53832017	4.49332607	4.48168907
0.6	5.63672018	5.31527448	5.11949465	5.00655421	4.95303242
0.7	6.63976350	6.11268126	5.78307572	5.58253976	5.47394739
0.8	7.80278633	7.02662119	6.53427685	6.22649621	6.04964746
0.9	9.13155046	8.06285606	7.37885987	6.94418536	6.68589444

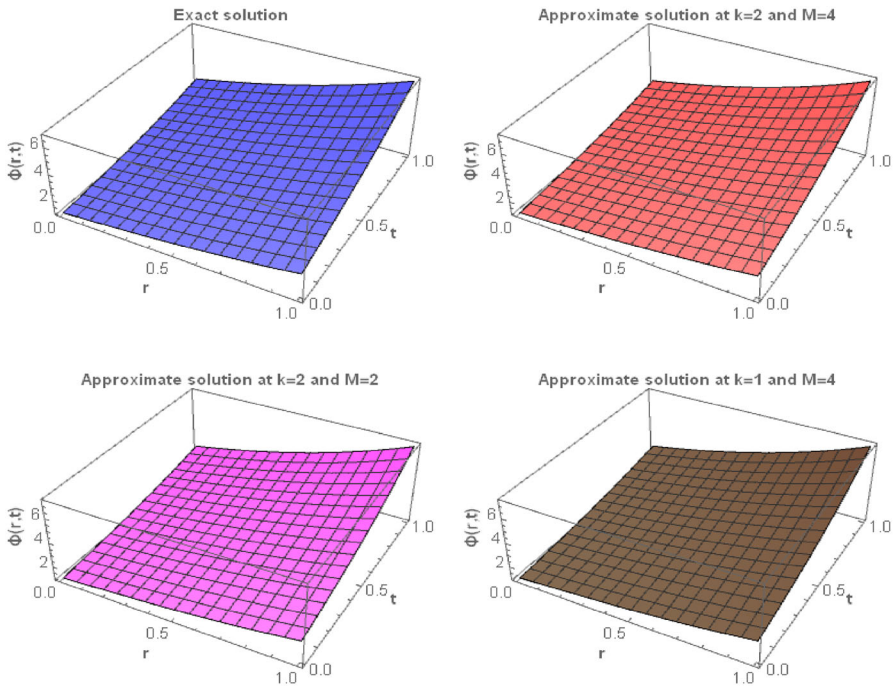


Fig. 3 Graphical representation of present method solution at different values of k and M and $\alpha = 1$, for example, 1

$$r_i = t_i = \frac{2i - 1}{2^k [M]^2}, i = 1, 2, \dots, 2^{k-1} [M]^2. \tag{5.11}$$

We solve the nonlinear system of algebraic equations using the Newton–Raphson method to ascertain the values of the unknown coefficients. In Eq. (5.9), substitute the obtained values of the unknown coefficients to get the deserved approximate solution for the given PDE.

Case II: Utilizing the notion of Caputo derivative, which is defined in Sect. 2.1, differentiate Eq. (5.9) fractionally of order $\alpha \in (0, 1)$ for the given equation. Then we obtain,

$$\begin{aligned} \frac{\partial^\alpha \Phi(r, t)}{\partial t^\alpha} &= \frac{d^\alpha}{dt^\alpha} G_2(t) + \frac{d^\alpha}{dt^\alpha} \left[\left[H' \omega(r) + \overline{\omega(r)} \right]^T \mathcal{Q} \left[H \omega(t) + \overline{\omega(t)} \right] \right] \\ &+ \frac{r}{c} \frac{d^\alpha}{dt^\alpha} \left[G_3(t) - G_2(t) - G_1(c) + G_1(0) - \lim_{r \rightarrow c} \left[H' \omega(r) + \overline{\omega(r)} \right]^T \mathcal{Q} \left[H \omega(t) + \overline{\omega(t)} \right] \right]. \end{aligned} \tag{5.12}$$

To collocate with the collocation points $r_i = t_i = \frac{2i-1}{2^k [M]^2}, i = 1, 2, \dots, 2^{k-1} [M]^2$, by replacing $\Phi, \frac{\partial^\alpha \Phi(r, t)}{\partial t^\alpha}, \Phi_r,$ and Φ_{rr} in (5.1). For finding the unknown coefficients by applying the Newton–Raphson method to the obtained system of nonlinear algebraic

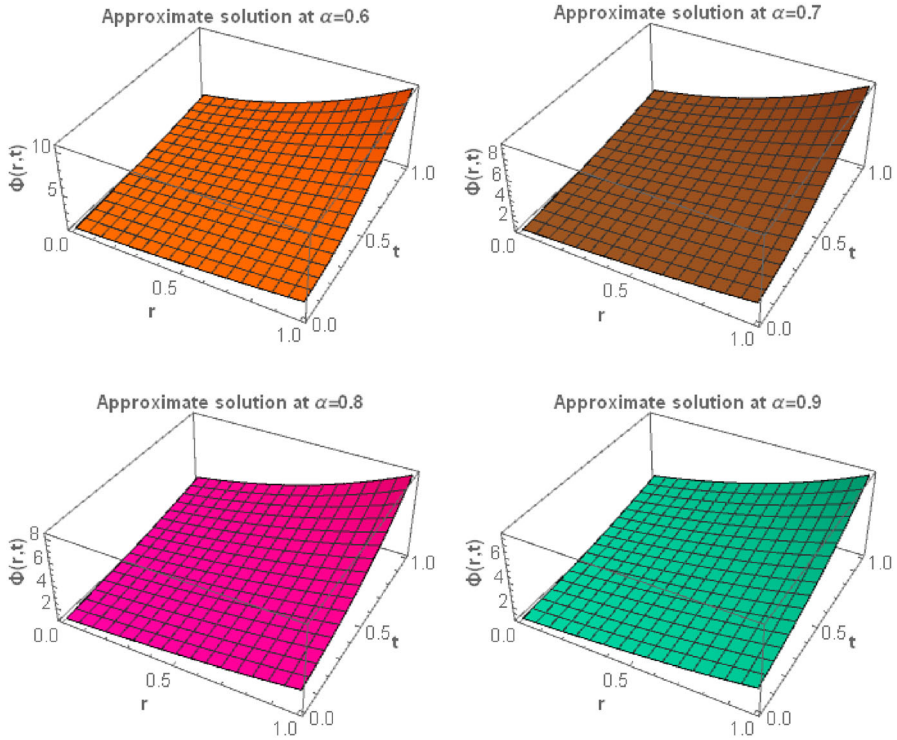


Fig. 4 Graphical interpretation of present technique solution at different values of α , for example, 1

Table 2 Present method solution for the different values of M at $r = 1$ and $\alpha = 1$, for example, 1

t	TWCM				
	$M = 2$	$M = 4$	$M = 6$	$M = 8$	$M = 10$
0.1	2.6390×10^{-5}	7.9038×10^{-6}	3.5958×10^{-7}	2.9215×10^{-7}	2.9215×10^{-7}
0.2	1.3100×10^{-4}	3.5087×10^{-5}	1.4816×10^{-6}	1.2017×10^{-6}	1.2017×10^{-6}
0.3	3.1986×10^{-4}	8.3030×10^{-5}	3.4246×10^{-6}	2.7761×10^{-6}	2.7761×10^{-6}
0.4	5.9961×10^{-4}	1.5336×10^{-4}	6.2530×10^{-6}	5.0674×10^{-6}	5.0674×10^{-6}
0.5	9.7760×10^{-4}	2.4790×10^{-4}	1.0038×10^{-5}	8.1334×10^{-6}	8.1334×10^{-6}
0.6	1.4619×10^{-3}	3.6863×10^{-4}	1.4858×10^{-5}	1.2037×10^{-5}	1.2037×10^{-5}
0.7	2.0616×10^{-3}	5.1776×10^{-4}	2.0801×10^{-5}	1.6851×10^{-5}	1.6851×10^{-5}
0.8	2.7865×10^{-3}	6.9773×10^{-4}	2.7963×10^{-5}	2.2651×10^{-5}	2.2651×10^{-5}
0.9	3.6476×10^{-3}	9.1123×10^{-4}	3.6449×10^{-5}	2.9524×10^{-5}	2.9524×10^{-5}

Table 3 Absolute error comparison of the present method with BPCM at $r = 1$, for example, 1

t	TWCM			
	$\alpha = 0.7$ at $M = 5$	$\alpha = 0.8$ at $M = 5$	$\alpha = 0.9$ at $M = 5$	$\alpha = 1$ at $M = 8$
0.1	9.3996×10^{-2}	5.4343×10^{-2}	2.4044×10^{-2}	2.9215×10^{-7}
0.3	9.6745×10^{-2}	6.4526×10^{-2}	3.2575×10^{-2}	2.7761×10^{-6}
0.5	1.4749×10^{-1}	5.6631×10^{-2}	1.1637×10^{-2}	8.1334×10^{-6}
0.7	6.3873×10^{-1}	3.0912×10^{-1}	1.0859×10^{-1}	1.6851×10^{-5}
0.9	0.1376×10^{-1}	6.9296×10^{-1}	2.5829×10^{-1}	2.9524×10^{-5}
	BPCM [21]			
0.1	2.7376×10^{-1}	1.4059×10^{-1}	4.5292×10^{-2}	1.7012×10^{-8}
0.3	6.2916×10^{-1}	3.6310×10^{-1}	1.4828×10^{-1}	1.5301×10^{-6}
0.5	8.8395×10^{-1}	5.2755×10^{-1}	2.2681×10^{-1}	1.5822×10^{-5}
0.7	0.1109×10^{-1}	6.7550×10^{-1}	2.9821×10^{-1}	1.5822×10^{-5}
0.9	0.1324×10^{-1}	8.1897×10^{-1}	3.6794×10^{-1}	2.7307×10^{-4}

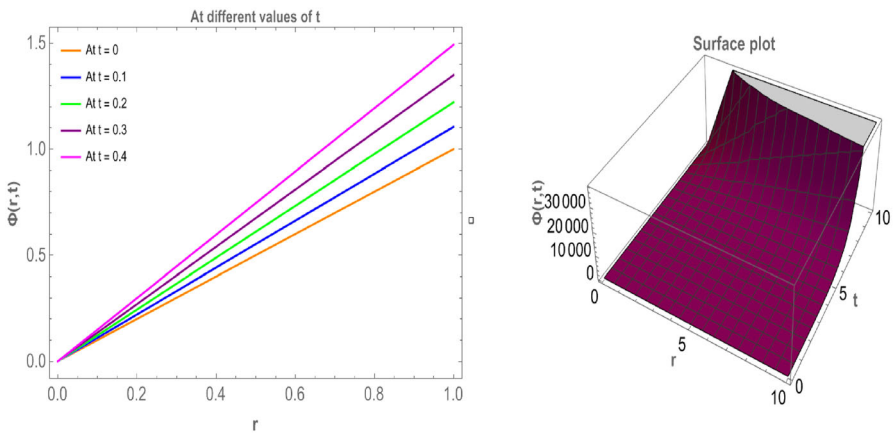


Fig. 5 The development of tumour cells in exponential form, for example, 2

equations. Substitute the calculated values for the unknown coefficients in Eq. (5.9), which produces the desired solution of the proposed method.

6 Potential implementations of the proposed methodology

To demonstrate the usefulness of the suggested technique, three different types of FBEs are tested, simulated, and compared.

Example 1 If $\Theta(r, t) = \frac{1}{2}\Phi(r, t)$, then the FBE (3.12) can be written as [21]

Table 4 Projected method solution for the different α values at $r = 1$, for example, 2

t	TWCM				
	$\alpha = 0.6$	$\alpha = 0.7$	$\alpha = 0.8$	$\alpha = 0.9$	$\alpha = 1$
0.1	0.95613287	1.01117449	1.05082720	1.08112672	1.10517091
0.2	1.02852108	1.09515795	1.14555029	1.18650017	1.22140275
0.3	1.21832788	1.25311366	1.28533256	1.31728362	1.34985880
0.4	1.52683893	1.48632724	1.47145964	1.47476271	1.49182469
0.5	1.95547507	1.79621955	1.70535237	1.66035827	1.64872127
0.6	2.50580655	2.18436086	1.98858103	1.87564059	1.82211880
0.7	3.17956882	2.65248658	2.32288103	2.12234508	2.01375270
0.8	3.97867980	3.20251465	2.71017032	2.40238968	2.22554092
0.9	4.90525913	3.83656473	3.15256853	2.71789403	2.45960311

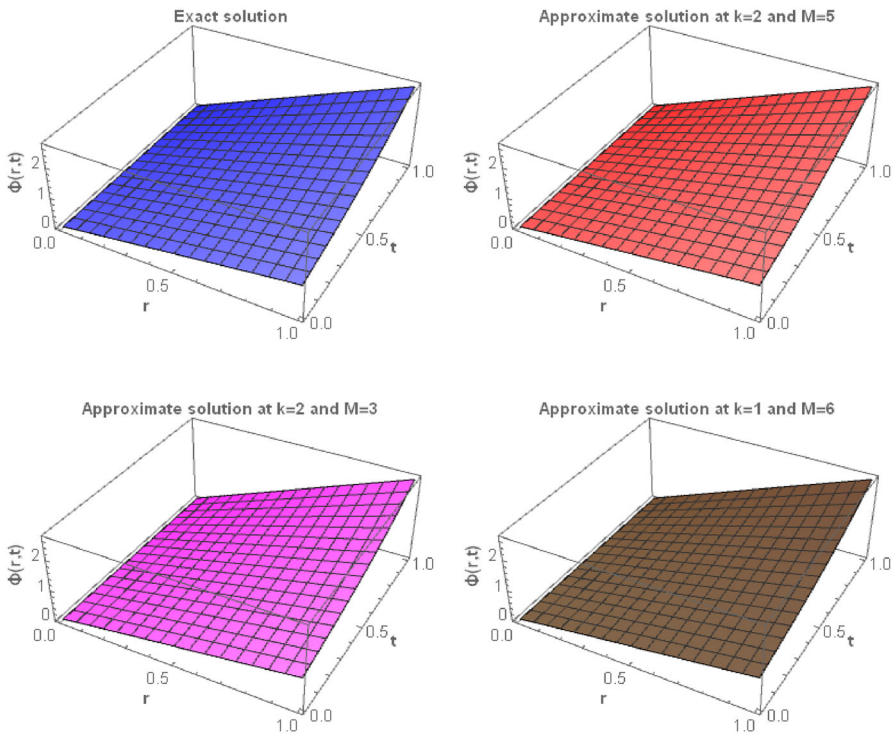


Fig. 6 Graphical interpretation of projected method solution at different values of k and M and $\alpha = 1$, for example, 2

Table 5 Absolute error for different values of k and M with setting $t = 1$, for example, 2

r	Exact solution	TWCM			
		$k = 1$ and $M = 2$	$k = 2$ and $M = 2$	$k = 1$ and $M = 4$	$k = 2$ and $M = 4$
0.1	0.27182818	1.5176×10^{-13}	1.0119×10^{-13}	4.4089×10^{-14}	5.9396×10^{-15}
0.2	0.54365636	9.1149×10^{-13}	4.4597×10^{-13}	1.0438×10^{-13}	2.1149×10^{-14}
0.3	0.81548454	2.6728×10^{-12}	1.0721×10^{-12}	3.6581×10^{-14}	1.6614×10^{-13}
0.4	1.08731273	5.7467×10^{-12}	1.9853×10^{-12}	3.5244×10^{-13}	5.3707×10^{-13}
0.5	1.35914091	1.0359×10^{-11}	3.1591×10^{-12}	1.3041×10^{-12}	1.2656×10^{-12}
0.6	1.63096909	1.6655×10^{-11}	4.5353×10^{-12}	3.1088×10^{-12}	2.5066×10^{-12}
0.7	1.90279727	2.4693×10^{-11}	6.0234×10^{-12}	6.1052×10^{-12}	4.4381×10^{-12}
0.8	2.17462546	3.4451×10^{-11}	7.5008×10^{-12}	1.0680×10^{-11}	7.2617×10^{-12}
0.9	2.44645364	4.5822×10^{-11}	8.8131×10^{-12}	1.7270×10^{-11}	1.1202×10^{-11}

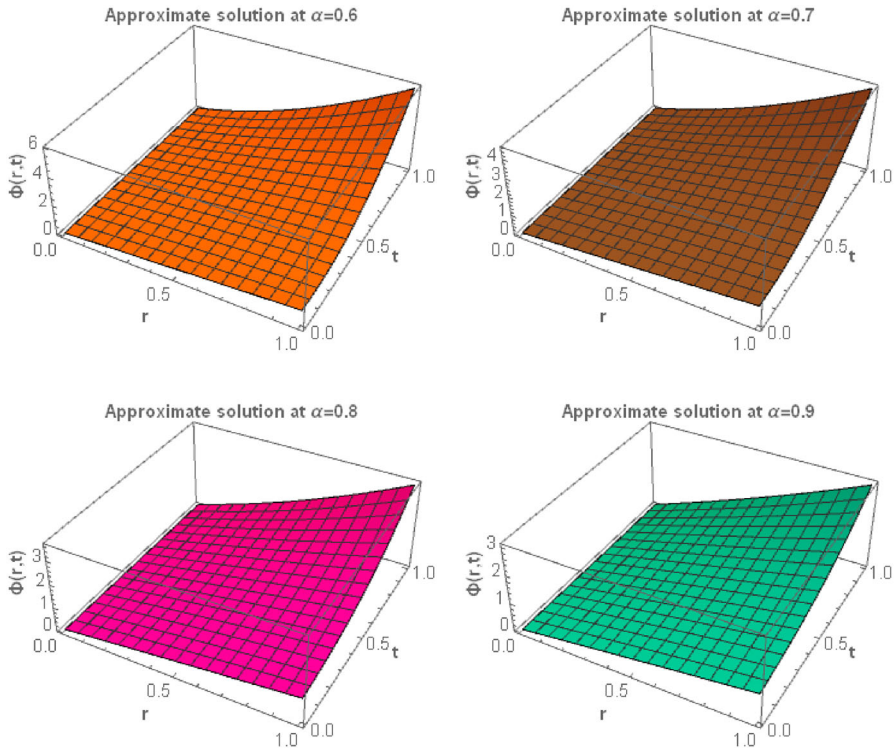


Fig. 7 Graphical judgement of present technique solution at different values of α , for example, 2

Table 6 Present method solution for the different values of M at $r = 1$ and $\alpha = 1$, for example, 2

t	TWCM				
	$M = 2$	$M = 4$	$M = 6$	$M = 8$	$M = 10$
0.1	2.6361×10^{-12}	3.0508×10^{-13}	5.2624×10^{-14}	4.4408×10^{-14}	4.4408×10^{-14}
0.2	2.7324×10^{-12}	1.1057×10^{-13}	1.9095×10^{-14}	4.6629×10^{-15}	4.6629×10^{-15}
0.3	5.3357×10^{-13}	5.6599×10^{-13}	9.9253×10^{-14}	1.1701×10^{-13}	1.1701×10^{-13}
0.4	3.7165×10^{-12}	1.7117×10^{-12}	3.0442×10^{-13}	3.1907×10^{-13}	3.1907×10^{-13}
0.5	9.7739×10^{-12}	3.3184×10^{-12}	5.9974×10^{-13}	6.0240×10^{-13}	6.0240×10^{-13}
0.6	1.7393×10^{-11}	5.3839×10^{-12}	9.9142×10^{-13}	9.7011×10^{-13}	9.7011×10^{-13}
0.7	2.6332×10^{-11}	7.9096×10^{-12}	1.4863×10^{-12}	1.4288×10^{-12}	1.4288×10^{-12}
0.8	3.6344×10^{-11}	1.0903×10^{-11}	2.0912×10^{-12}	1.9868×10^{-12}	1.9868×10^{-12}
0.9	4.7187×10^{-11}	1.4378×10^{-11}	2.8093×10^{-12}	2.6578×10^{-12}	2.6578×10^{-12}

Table 7 Absolute error comparison of the present method with BPCM at $r = 1$, for example, 2

t	TWCM			
	$\alpha = 0.7$	$\alpha = 0.8$	$\alpha = 0.9$	$\alpha = 1$
0.1	9.3996×10^{-2}	5.4343×10^{-2}	2.4044×10^{-2}	2.6361×10^{-12}
0.3	9.6745×10^{-2}	6.4526×10^{-2}	3.2575×10^{-2}	5.3357×10^{-13}
0.5	1.4749×10^{-1}	5.6631×10^{-2}	1.1637×10^{-2}	9.7739×10^{-12}
0.7	6.3873×10^{-1}	6.3873×10^{-1}	1.0859×10^{-1}	2.6332×10^{-11}
0.9	0.1376×10^{-1}	6.9296×10^{-1}	2.5829×10^{-1}	4.7187×10^{-11}
	BPCM [21]			
0.1	9.4391×10^{-2}	4.9615×10^{-2}	1.6373×10^{-2}	1.9153×10^{-10}
0.3	1.9583×10^{-1}	1.1740×10^{-1}	4.9677×10^{-2}	1.4277×10^{-8}
0.5	2.5214×10^{-1}	1.5740×10^{-1}	7.0724×10^{-2}	1.0309×10^{-7}
0.7	2.9199×10^{-1}	1.8654×10^{-1}	8.6557×10^{-2}	4.0083×10^{-7}
0.9	3.2294×10^{-1}	2.0978×10^{-1}	9.9400×10^{-2}	1.1403×10^{-6}

$$\frac{\partial^\alpha \Phi(r, t)}{\partial t^\alpha} = \frac{1}{2} \Phi(r, t) + \frac{1}{2} \frac{\partial^2 \Phi(r, t)}{\partial r^2},$$

with initial condition

$$\Phi(r, 0) = e^r.$$

The analytical solution of the given FBE is $\Phi(r, t) = e^{r+t}$ for $\alpha = 1$. This problem is solved by the projected technique TWCM. As time passes, the radius and density

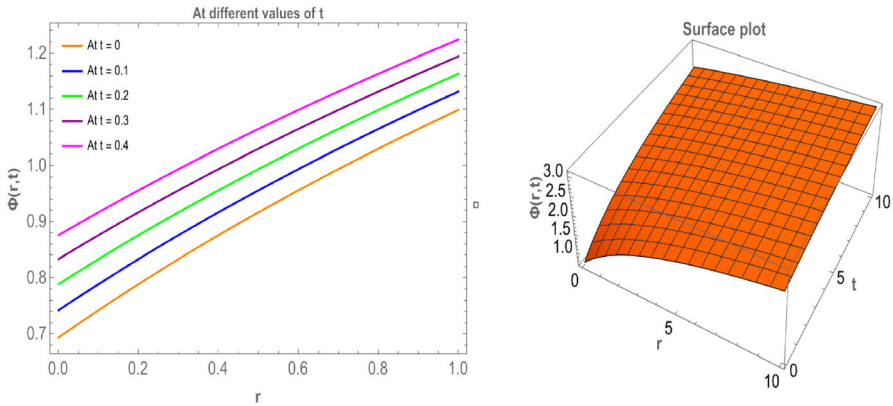


Fig. 8 The development of tumour cells, for example, 3

Table 8 Projected method solution for the different α values at $r = 0.1$, for example, 3

t	TWCM				
	$\alpha = 0.6$	$\alpha = 0.7$	$\alpha = 0.8$	$\alpha = 0.9$	$\alpha = 1$
0.1	0.78631890	0.78682656	0.78742420	0.78811895	0.78845736
0.2	0.82797299	0.82888541	0.82996148	0.83122136	0.83290912
0.3	0.86828310	0.86949738	0.87093267	0.87262805	0.87546873
0.4	0.90740180	0.90881504	0.91049034	0.91249161	0.91629073
0.5	0.94546387	0.94697316	0.94876927	0.95094680	0.95551144
0.6	0.98258892	0.98409137	0.98588907	0.98811324	0.99325177
0.7	1.01888360	1.02027630	1.02195639	1.02409757	1.02961941
0.8	1.05444341	1.05562346	1.05706673	1.05899530	1.06471073
0.9	1.08935417	1.09021867	1.09130591	1.09289225	1.09861228

of the affected person’s tumour cells increase, as plotted in Fig. 2. Figure 2 exhibits the tumour cells developing exponentially at a constant rate. Table 1 gives the projected method solution for different values of α at $M = 5$. Figure 3 explains the graphical presentation of the present method solution by varying values of k and M for integer order. Figure 4 displays the graph of the fractional order solution of our method at different values of α . Table 2 shows the present method solution at different values of M . From Table 2, we observed the stability of example 1 at $M = 8$, and after increasing M , the solution by the present approach becomes stable. The present method solution is compared with the Bernoulli polynomial collocation method (BPCM) [21] at different values of α in Table 3. We used Mathematica software to simulate these problems.

Example 2 If $\Theta(r, t) = \Phi(r, t)$, then the FBE (3.12) can be written as [21]

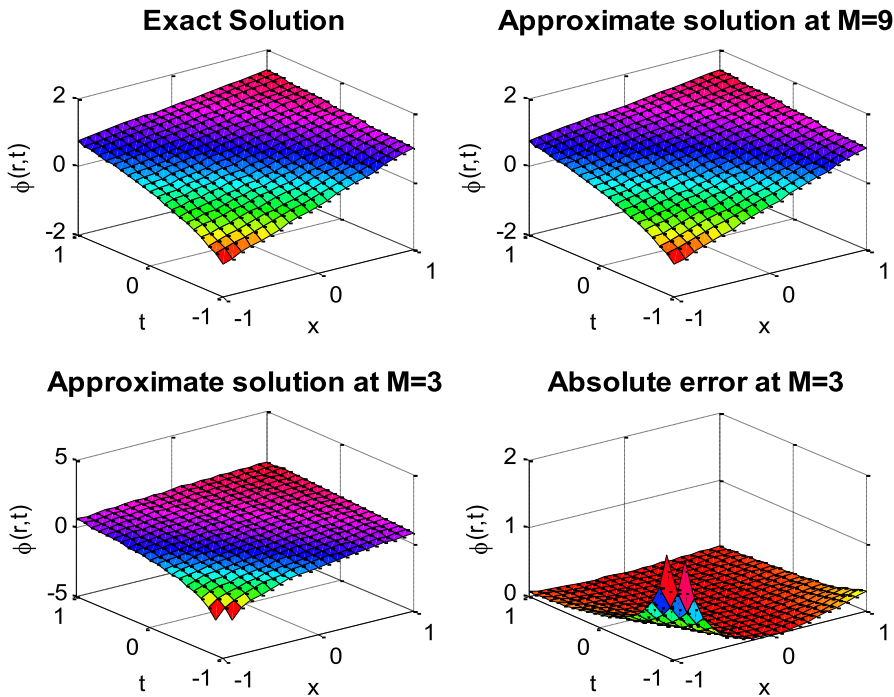


Fig. 9 Graphical presentation of projected method solution at different values of k and M and $\alpha = 1$, for example, 3

$$\frac{\partial^\alpha \Phi(r, t)}{\partial t^\alpha} = \Phi(r, t) + \frac{1}{2} \frac{\partial^2 \Phi(r, t)}{\partial r^2},$$

with initial condition

$$\Phi(r, 0) = r.$$

The analytical solution of the given FBE is $\Phi(r, t) = re^t$ for $\alpha = 1$. Applying the suggested method and choosing different values of M allows for the solution to this problem. Figure 5 demonstrates as time goes on, the radius and density of tumour cells of the affected person increase, and the tumour cells mature in the exponential form. For the fractional order α , we solved this problem by using Taylor wavelets, and numerical values are given in Table 4 at $M = 2$. Figure 6 shows the graphical interpretation of the suggested method solution at different values of k and M for $\alpha = 1$. Table 5 compares absolute errors for different values of k and M . Figure 7 shows the graphical exhibition of the projected technique solution at different α values. Table 6 gives the stability of example 2 by varying the value of M . At some instant of M and increasing value of M , the solution becomes stable and unchanged. Table 7 compares the present technique with the literature method BPCM [21] at $M = 2$.

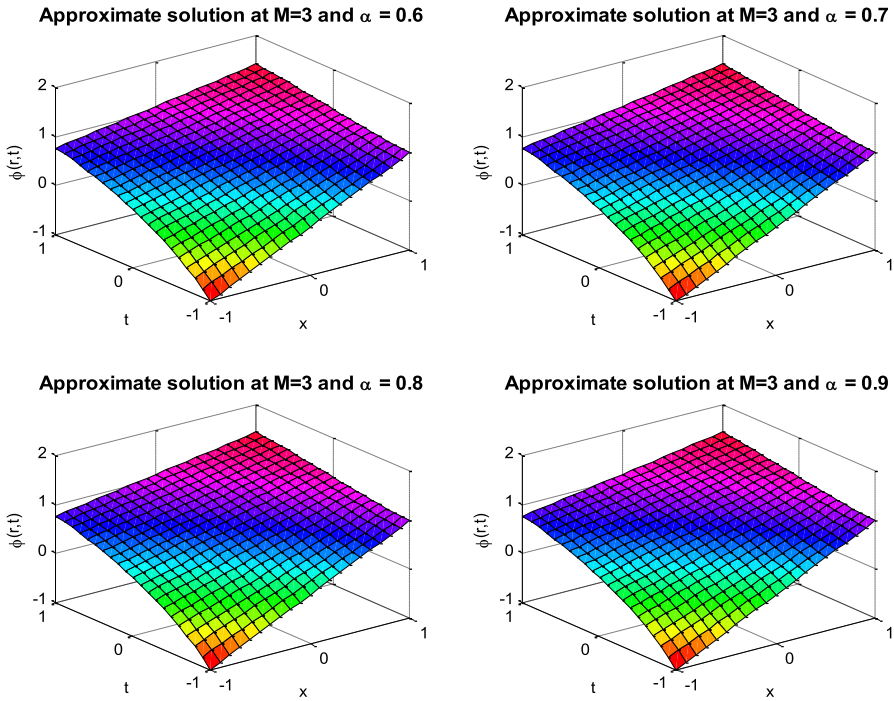


Fig. 10 Graphical judgement of present technique solution at different values of α , for example, 3

Table 9 Present method solution for the different values of M at $r = 0.1$ and $\alpha = 1$, for example, 3

t	TWCM				
	$M = 2$	$M = 3$	$M = 6$	$M = 8$	$M = 10$
0.0	9.6039×10^{-5}	9.7313×10^{-6}	5.0000×10^{-12}	5.0000×10^{-12}	5.0000×10^{-12}
0.1	1.9227×10^{-4}	3.7708×10^{-6}	5.1746×10^{-9}	5.1748×10^{-9}	5.1738×10^{-9}
0.2	4.6602×10^{-4}	6.6882×10^{-5}	4.1364×10^{-8}	4.1364×10^{-8}	4.1357×10^{-8}
0.3	7.2766×10^{-4}	1.9662×10^{-4}	1.3959×10^{-7}	1.3959×10^{-7}	1.3957×10^{-7}
0.4	9.7913×10^{-4}	3.9104×10^{-4}	3.3088×10^{-7}	3.3088×10^{-7}	3.3082×10^{-7}
0.5	1.2220×10^{-3}	6.4856×10^{-4}	6.4624×10^{-7}	6.4625×10^{-7}	6.4613×10^{-7}
0.6	1.4576×10^{-3}	9.6791×10^{-4}	1.1167×10^{-6}	1.1167×10^{-6}	1.1165×10^{-6}
0.7	1.6869×10^{-3}	1.3480×10^{-3}	1.7733×10^{-6}	1.7733×10^{-6}	1.7730×10^{-6}
0.8	1.9108×10^{-3}	1.7881×10^{-3}	2.6470×10^{-6}	2.6470×10^{-6}	2.6465×10^{-6}
0.9	2.1301×10^{-3}	2.2873×10^{-3}	3.7688×10^{-6}	3.7689×10^{-6}	3.7682×10^{-6}
1.0	2.3453×10^{-3}	2.8451×10^{-3}	5.1699×10^{-6}	5.1700×10^{-6}	5.1690×10^{-6}

Table 10 Absolute error comparison of the present method with BPCM at $r = 1$, for example, 3

t	TWCM			
	$\alpha = 0.7$ at $M = 3$	$\alpha = 0.8$ at $M = 3$	$\alpha = 0.9$ at $M = 3$	$\alpha = 1$ at $M = 6$
0.1	2.1474×10^{-5}	1.5903×10^{-5}	6.6355×10^{-5}	3.7708×10^{-9}
0.3	1.2326×10^{-4}	1.1824×10^{-4}	1.5273×10^{-4}	1.3959×10^{-7}
0.5	2.1636×10^{-4}	2.1244×10^{-4}	2.9336×10^{-4}	6.4624×10^{-7}
0.7	3.0088×10^{-4}	2.9861×10^{-4}	4.8812×10^{-4}	1.7733×10^{-6}
0.9	3.7691×10^{-4}	3.7684×10^{-4}	7.3694×10^{-4}	3.7688×10^{-6}
	BPCM [21]			
0.1	2.8170×10^{-2}	1.4556×10^{-2}	4.5496×10^{-3}	7.6955×10^{-10}
0.3	4.9831×10^{-2}	2.8885×10^{-2}	1.1664×10^{-2}	2.2897×10^{-5}
0.5	6.0230×10^{-2}	3.2774×10^{-2}	1.3337×10^{-2}	5.6819×10^{-6}
0.7	8.3800×10^{-2}	3.8679×10^{-2}	1.4396×10^{-2}	6.5341×10^{-4}
0.9	1.3976×10^{-1}	5.8018×10^{-2}	2.0070×10^{-2}	3.7621×10^{-3}

Example 3 If $\Theta(r, t) = e^{-\Phi(r,t)} + \frac{1}{2}e^{-2\Phi(r,t)}$, then the FBE (3.12) can be written as [21]

$$\frac{\partial^\alpha \Phi(r, t)}{\partial t^\alpha} = e^{-\Phi(r,t)} + \frac{1}{2}e^{-2\Phi(r,t)} + \frac{1}{2} \frac{\partial^2 \Phi(r, t)}{\partial r^2},$$

with initial condition

$$\Phi(r, 0) = \ln(r + 2).$$

The analytical solution of the given FBE is $\Phi(r, t) = \ln(r + t + 2)$ for $\alpha = 1$. This problem can be solved using the suggested approach. The graphical analysis of the growth profile of tumour cells at different times is plotted in Fig. 8. This figure reveals that, with increasing time tumour exponential growth. Table 8 gives the current approach solution for different values of α at $M = 3$. Figure 9 shows the graphical judgement of the present method solution at different values of k and M for $\alpha = 1$. Figure 10 shows the graphical exhibition of the projected technique solution at different values of α . The stability of example 3 can be observed in Table 9 by varying the values of M . Table 10 provides a comparison between the current approach and BPCM [21]. Therefore, even if PDE is nonlinear, the suggested method works well.

7 Conclusion

A developing area of science is mathematical diffusive modelling for glioma growth and invasion simulation. The research on glioblastoma brain tumour cells has been very beneficial in addressing issues related to the formation of gliomas, their formal genesis, growth, and diffusion, and treatments provided that they exist as a cell type, and clear evidence will be supplied. The most typical primary brain tumour in adults, glioblastoma, often have a short survival time. Chemotherapy, radiation therapy, and surgery are the usual methods of treating brain tumours. In recent years, mathematical models have been used to research untreated and treated brain tumours. This study considered the fractional Burgess equation in terms of Caputo. A method is suggested to solve the model being studied due to the model itself. By using the properties of Taylor wavelets, we create this method. Finally, the study's model is simulated, evaluated, and compared using the suggested technique. With minor modifications to this method, the current approach can be extended to mathematical models with higher-order PDEs, higher-order fractional PDEs, time-delay PDEs, and systems of PDEs.

Acknowledgements The author expresses his affectionate thanks to the DST-SERB, Govt. of India. New Delhi for the financial support under Empowerment and Equity Opportunities for Excellence in Science for 2023-2026. F.No.EEQ/2022/620 Dated:07/02/2023.

Availability of Data and Materials The data that support the findings of this study are available within the article.

Declarations

Conflict of interest The authors declare that they have no conflict of interest.

Ethical approval This article contains no studies with human participants or animals performed by authors.

References

1. Baleanu, D., S. Sadat Sajjadi, A. Jajarmi, and J.H. Asad. 2019. New features of the fractional Euler-Lagrange equations for a physical system within non-singular derivative operator. *The European Physical Journal Plus*. 134: 181.
2. Baleanu, D., A. Jajarmi, S.S. Sajjadi, and D. Mozyrska. 2019. A new fractional model and optimal control of a tumor-immune surveillance with non-singular derivative operator. *Chaos: An Interdisciplinary Journal of Nonlinear Science*. 29 (8): 083127.
3. Saad, K.M., A. Atangana, and D. Baleanu. 2018. New fractional derivatives with non-singular kernel applied to the Burgers equation. *Chaos: An Interdisciplinary Journal of Nonlinear Science*. 28 (6): 063109.
4. Kilbas, A.A., H.M. Srivastava, and J.J. Trujillo. 2006. *Theory and applications of fractional differential equations*. Amsterdam: Elsevier.
5. Sabatier, J., O.P. Agrawal, and J.A.T. Machado. 2007. *Advances in fractional calculus: theoretical developments and applications in physics and engineering*. Dordrecht: Springer.
6. Samko, S.G., A.A. Kilbas, and O.I. Marichev. 1993. *Fractional Integrals and Derivatives: theory and Applications*. Switzerland: Gordon and Breach.
7. Podlubny, I. 1999. *Fractional differential equations*. San Diego: Academic Press.

8. Atangana, A., and D. Baleanu. 2016. New fractional derivatives with nonlocal and non-singular kernel: theory and application to heat transfer model. *Thermal Science*. 20 (2): 763–769.
9. Caputo, M., and M. Fabrizio. 2015. A new definition of fractional derivative without singular kernel. *Progress in Fractional Differentiation and Applications*. 1 (2): 73–85.
10. Schiffer, D., L. Annovazzi, V. Caldera, and M. Mellai. 2010. On the origin and growth of gliomas. *Anticancer Research*. 30 (6): 1977–1998.
11. Alvord, E.C., Jr., and C.M. Shaw. 1991. Neoplasms affecting the nervous system of the elderly. In *The Pathology of the Aging Human Nervous System*, ed. S. Duckett, 210–286. Philadelphia: Lea and Fabiger.
12. Silbergeld, D.L., R.C. Rostomily, and E.C. Alvord Jr. 1991. The cause of death in patients with glioblastoma is multifactorial: clinical factors and autopsy findings in 117 cases of supratentorial glioblastoma in adults. *Journal Neuro-Oncology*. 10: 179–185.
13. Blankenberg, F.G., R.L. Teplitz, W. Ellis, M.S. Salamat, B.H. Min, L. Hall, et al. 1995. The influence of volumetric tumor doubling time, DNA ploidy, and histologic grade on the survival of patients with intracranial astrocytomas. *American Journal of Neuroradiology*. 16: 1001–1012.
14. Shuman, R.M., E.C. Alvord Jr., and R.W. Leech. 1975. The biology of childhood ependymomas. *Archives of Neurology*. 32: 731–739.
15. Silbergeld, D.L., and M.R. Chicoine. 1997. Isolation and characterization of human malignant glioma cells from histologically normal brain. *Journal of Neurosurgery*. 86: 525–531.
16. Burgess, P.K., P.M. Kulesa, J.D. Murray, and E.C. Alvord. 1997. The interaction of growth rates and diffusion coefficients in a three-dimensional mathematical model of gliomas. *Journal of Neuropathology and Experimental Neurology*. 56: 704–713.
17. Tracqui, P., G.C. Cruywagen, D.E. Woodward, G.T. Bartoo, J.D. Murray, and J.R. Alvord. 1995. A mathematical model of glioma growth: the effect of chemotherapy on spatio-temporal growth. *Cell Proliferation*. 28: 17–31.
18. Woodward, D.E., J. Cook, P. Tracqui, G.C. Cruywagen, J.D. Murray, and J.R. Alvord. 1996. A mathematical model of glioma growth: the effect of extent of surgical resection. *Cell Proliferation*. 29: 269–288.
19. Cruywagen, G.C., D.E. Woodward, P. Tracqui, G.T. Bartoo, J.D. Murray, and E.C. Alvord. 1995. The modeling of diffusive tumours. *Journal of Biological Systems*. 3: 937–945.
20. González-Gaxiola, O., and R. Bernal-Jaquez. 2017. Applying adomian decomposition method to solve Burgess equation with a non-linear source. *International Journal of Applied and Computational Mathematics*. 3 (1): 213–224.
21. Ganji, R.M., H. Jafari, S.P. Moshokoa, and N.S. Nkomo. 2021. A mathematical model and numerical solution for brain tumor derived using fractional operator. *Results in Physics*. 28: 104671.
22. Swanson, K.R., C. Bridge, J.D. Murray, and E.C. Alvord Jr. 2003. *Virtual and real brain tumors: using mathematical modeling to quantify glioma growth and invasion*. 216 (1): 1–10.
23. Murray, J.D. 1993. *Mathematical biology*. New York: Springer.
24. Kumbinaraiaiah, S., and M. Mulimani. 2022. A novel scheme for the hyperbolic partial differential equation through Fibonacci wavelets. *Journal of Taibah University for Science*. 16 (1): 1112–1132.
25. Kumbinaraiaiah, S., and M. Mulimani. 2023. Fibonacci wavelets-based numerical method for solving fractional order $(1 + 1)$ -dimensional dispersive partial differential equation. *International Journal of Dynamics and Control*. 11: 2232–2255.
26. Singh, S., V.K. Patel, and V.K. Singh. 2018. Application of wavelet collocation method for hyperbolic partial differential equations via matrices. *Applied Mathematics and Computation*. 320: 407–424.
27. Kumbinaraiaiah, S., and M. Mulimani. 2023. Bernoulli wavelets numerical approach for the nonlinear Klein–Gordon and Benjamin–Bona–Mahony equation. *International Journal of Applied and Computational Mathematics*. 9 (5): 108.
28. Kumbinaraiaiah, S., G. Manohara, and G. Hariharan. 2023. Bernoulli wavelets functional matrix technique for a system of nonlinear singular Lane Emden equations. *Mathematics and Computers in Simulation*. 204: 133–165.
29. Kumbinaraiaiah, S., and M. Mulimani. 2023. A study on the non-linear murray equation through the bernoulli wavelet approach. *International Journal of Applied and Computational Mathematics*. 9 (3): 40.
30. Priyadarshi, G., and B.V. Rathish Kumar. 2021. Reconstruction of the parameter in parabolic partial differential equations using Haar wavelet method. *Engineering Computations*. 38 (5): 2415–2433.
31. Aruldoss, R., R.A. Devi, and P.M. Krishna. 2021. An expeditious wavelet-based numerical scheme for solving fractional differential equations. *Computational and Applied Mathematics*. 40 (1): 2.

32. Manohara, G., and S. Kumbinaraiaiah. 2024. Numerical solution of some stiff systems arising in chemistry via Taylor wavelet collocation method. *Journal of Mathematical Chemistry*. 62: 24–61.
33. Shiralashetti, S.C., and S. Kumbinaraiaiah. 2017. Theoretical study on continuous polynomial wavelet bases through wavelet series collocation method for nonlinear Lane–Emden type equations. *Applied Mathematics and Computation*. 315: 591–602.
34. Toan, P.T., T.N. Vo, and M. Razzaghi. 2021. Taylor wavelet method for fractional delay differential equations. *Engineering with Computers* 37: 231–240.
35. Vo, T.N., M. Razzaghi, and P.T. Toan. 2022. Fractional-order generalized Taylor wavelet method for systems of nonlinear fractional differential equations with application to human respiratory syncytial virus infection. *Soft Computing*. 26: 165–173.
36. Keshavarz, E., and Y. Ordokhani. 2019. A fast numerical algorithm based on the Taylor wavelets for solving the fractional integro-differential equations with weakly singular kernels. *Mathematical Methods in the Applied Sciences*. 42 (13): 4427–4443.
37. Korkut, S.Ö. 2023. An accurate and efficient numerical solution for the generalized Burgers–Huxley equation via Taylor wavelets method: qualitative analyses and applications. *Mathematics and Computers in Simulation*. 209: 324–341.
38. Keshavarz, E., Y. Ordokhani, and M. Razzaghi. 2018. The Taylor wavelets method for solving the initial and boundary value problems of Bratu-type equations. *Applied Numerical Mathematics*. 128: 205–216.
39. Gümgüm, S. 2020. Taylor wavelet solution of linear and nonlinear Lane-Emden equations. *Applied Numerical Mathematics*. 158: 44–53.
40. Mulimani, M., and S. Kumbinaraiaiah. 2023. Numerical solution of time-fractional telegraph equations using wavelet transform. *International Journal of Dynamics and Control*. <https://doi.org/10.1007/s40435-023-01318-y>.
41. Avazzadeh, Z., H. Hassani, M.J. Ebadi, P. Agarwal, M. Poursadeghfard, and E. Naraghirad. 2023. Optimal approximation of fractional order brain tumor model using generalized laguerre polynomials. *Iranian Journal of Science*. 47: 501–513.
42. Masti, I., K. Sayevand, and H. Jafari. 2024. On analyzing two dimensional fractional order brain tumor model based on orthonormal Bernoulli polynomials and Newton’s method. *An International Journal of Optimization and Control: Theories & Applications*. 14 (1): 12–19.
43. Zureigat, H., M. Al-Smadi, A. Al-Khateeb, S. Al-Omari, and S. Alhazmi. 2023. Numerical solution for fuzzy time-fractional cancer tumor model with a time-dependent net killing rate of cancer cells. *International Journal of Environmental Research and Public Health*. 20 (4): 3766.
44. Padder, A., L. Almutairi, S. Qureshi, A. Soomro, A. Afroz, E. Hincal, and A. Tassaddiq. 2023. Dynamical analysis of generalized tumor model with Caputo fractional-order derivative. *Fractal and Fractional*. 7 (3): 258.
45. Al-Shomrani, M.M., and M.A. Abdelkawy. 2020. Numerical simulation for fractional-order differential system of a Glioblastoma Multiforme and Immune system. *Advances in Continuous and Discrete Models*. 2020: 516.
46. Kumbinaraiaiah, S., and M. Mulimani. 2023. Fibonacci wavelets approach for the fractional Rosenau–Hyman equations. *Results in Control and Optimization*. 11: 100221.

Publisher’s Note Springer Nature remains neutral with regard to jurisdictional claims in published maps and institutional affiliations.

Springer Nature or its licensor (e.g. a society or other partner) holds exclusive rights to this article under a publishing agreement with the author(s) or other rightsholder(s); author self-archiving of the accepted manuscript version of this article is solely governed by the terms of such publishing agreement and applicable law.